Results from NA49

C. Höhne[a] (for the NA49* Collaboration)

[a]Gesellschaft für Schwerionenforschung (GSI), Darmstadt, Germany

An overview of results from the CERN experiment NA49 is presented with emphasis on most recent measurements. NA49 has systematically studied the dependence of hadron production on energy and system size or centrality. At top-SPS energy the detailed investigation of hadron production, now also extending to elliptic flow of Λ-baryons and to identified particle yields at high p_t, shows that the created matter behaves in a similar manner as at RHIC energies. In the lower SPS energy range a distinct structure is observed in the energy dependence of the rate of strangeness production and in the slopes of p_t-spectra suggesting the onset of the creation of a deconfined phase of matter.

1. INTRODUCTION

Over the 9 years of data taking at the CERN-SPS (1994-2002), NA49 has collected a comprehensive set of data on hadron production in A+A collisions aiming at an understanding of the reaction mechanism through a systematic study of many observables in different systems and at different energies. Distinct changes of hadron production properties are expected once a deconfined phase of matter is created in the early stage of the collision.

Main observables in addition to a large variety of particle correlation and fluctuation measures were the hadro-chemical composition of the final state, in particular the strangeness content. The most extensive studies were performed for central Pb+Pb collisions at the top-SPS beam energy of 158A GeV, partially also extending to larger impact parameters and smaller collision systems. For many observables the energy dependence was studied over the full SPS energy range now providing a nearly continuous coverage from threshold to RHIC energies. This energy scan revealed that the SPS energy range is a particularly interesting region showing signs for the onset of deconfinement.

The NA49 detector [1] is a large acceptance hadron spectrometer. Main components are four large volume time projection chambers, two of them being located inside a magnetic field. Particle identification is done by a measurement of the specific energy loss in the TPCs, the time-of-flight around midrapidity, and by the study of decay topology and invariant mass. The centrality of the collisions is determined from the spectator energy measured in a forward calorimeter downstream of the spectrometer. The corresponding number of wounded nucleons $N_{\rm wound}$ and participating nucleons $N_{\rm part}$ is extracted by simulations based on the VENUS model [2]. In contrast to the calculation of $N_{\rm wound}$, nucleons participating through secondary cascading processes are also included in $N_{\rm part}$.

*For the full NA49 authors and acknowledgements, see appendix 'Collaborations' of this volume.

2. HADRON PRODUCTION AT 158A GeV BEAM ENERGY

In central Pb+Pb collisions at 158A GeV beam energy matter of high energy density, certainly exceeding 1 GeV/fm^3, is created at the early stage of the collision [3]. The yields of produced hadrons can successfully be described by hadron gas models, see *e.g.* [4,5], requiring temperatures of the order of 160 MeV, a baryochemical potential of about 240 MeV and, depending on the model, a strangeness undersaturation factor γ_s. These conditions show that the hadrochemical freeze-out occurs close to the predicted phase boundary [6] as is also the case for collisions at the higher RHIC energies [7]. It can be argued that already this is an indication that a deconfined state is created prior to freeze-out [8,9].

An effect of the higher baryon densities reached at top-SPS energies compared to RHIC is *e.g.* seen in the centrality dependence of midrapidity proton and antiproton yields normalized to the number of wounded nucleons (fig. 1). A slow increase is observed for protons which can be understood as a consequence of the increased stopping in central collisions. On the other hand, antiproton yields show a slight decrease which could be a sign of increasing antiproton absorption.

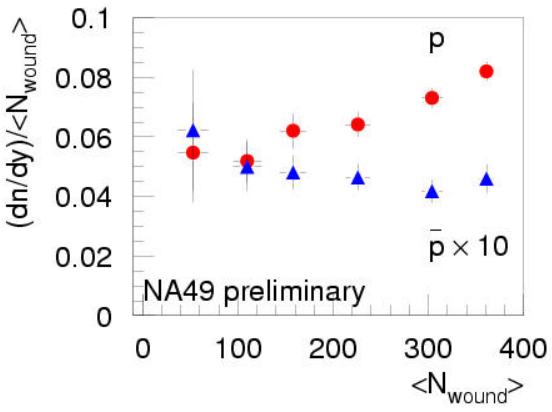

Figure 1. Proton and antiproton yields at midrapidity ($2.4 < y < 2.8$) normalized to the number of wounded nucleons $N_{\rm wound}$ versus centrality for Pb+Pb collisions at 158A GeV.

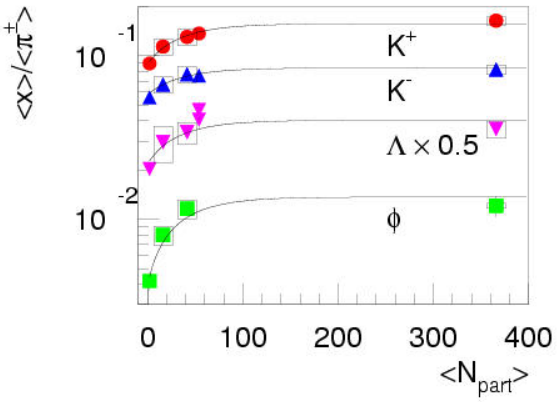

Figure 2. Strange hadron yields in 4π normalized to pions ($\langle\pi^{\pm}\rangle = \frac{\langle\pi^{+}\rangle+\langle\pi^{-}\rangle}{2}$) for increasingly large collision systems (p+p, central C+C, Si+Si, S+S and Pb+Pb) [10]; lines are to guide the eye.

In contrast, a fast increase with system size is observed for relative strangeness production (see fig. 2) reaching a saturation at about 60 participants [10]; similar results are also observed at RHIC for the centrality dependence of Au+Au collisions [11]. Although this phenomenon is qualitatively expected from statistical models due to strangeness suppression in small volumes, it cannot be explained quantitatively assuming a simple proportionality between volume and number of participants [12]. However, if one assumes several coherence volumes in the small collision systems as suggested by percolation calculations, the rise over a larger range of $N_{\rm part}$ in the data can be described also quantitatively [13].

Within such a percolation picture the observed increase of $\langle p_t \rangle$ and multiplicity fluctuations (fig. 3 and 4) towards smaller collision systems can also be understood [14]. Dynamical fluctuations would increase in the presence of several differently sized clusters but would be small if essentially a single string (p+p) or one large cluster (central Pb+Pb) existed. Assuming the known correlation of $\langle p_t \rangle$ and charged multiplicity in p+p reactions also for A+A collisions, the observed $\langle p_t \rangle$ fluctuations can be derived from the measured multiplicity fluctuations [16]. A similar centrality dependence of $\langle p_t \rangle$ fluctuations was observed at RHIC energies [17].

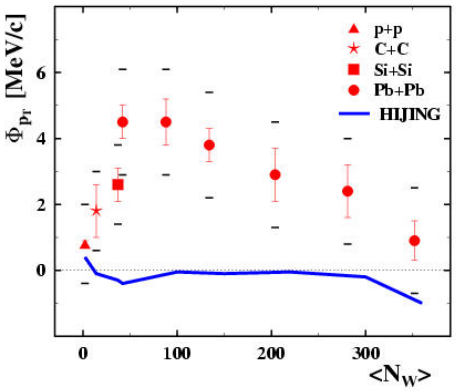

Figure 3. ϕ_{p_t} measure of $\langle p_t \rangle$ fluctuations for negatively charged particles versus system size (p+p, central C+C, Si+Si, Pb+Pb) and centrality (Pb+Pb) at 158A GeV ($4 < y_\pi < 5.5$) [15].

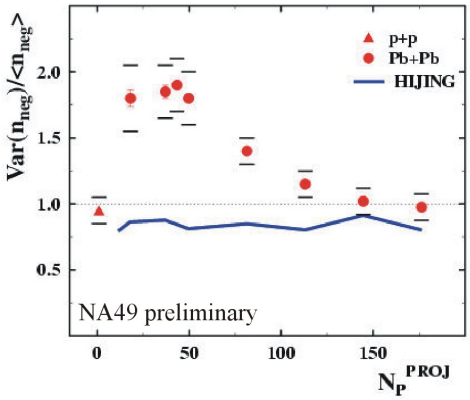

Figure 4. Multiplicity fluctuations for negatively charged particles versus centrality for Pb+Pb collisions at 158A GeV beam energy ($4 < y_\pi < 5.5$).

Additional information on the reaction mechanism can be extracted from the analysis of particle correlations, *e.g.* via the charge balance function. Similar to what has been measured at RHIC [18], NA49 observes a decrease of the width of the balance function for charged particles towards central Pb+Pb collisions. This is consistent with a delayed hadronization scenario in central Pb+Pb compared to collisions of larger impact parameter or of smaller systems [19]. Such a scenario is also supported by an analysis of chemical and kinetic freeze-out conditions in the smaller systems [20]. Separate measurements of the width at midrapidity and at forward rapidities (fig. 5) reveal that the narrowing effect is located at midrapidity.

Recently, NA49 also started to investigate observables which so far have been the domain of RHIC as *e.g.* elliptic flow of strange particles or high-p_t phenomena. Remarkably, the similarities between the matter created at top-SPS and RHIC also extend to these observations: In Pb+Pb collisions at 158A GeV a substantial elliptic flow for Λ-baryons is found which is similar to that of protons but clearly smaller than that of pions [21]. The measurement of particle yields at high p_t shows a strong increase of the baryon/meson ratio at $p_t > 2.5$ GeV/c [22].

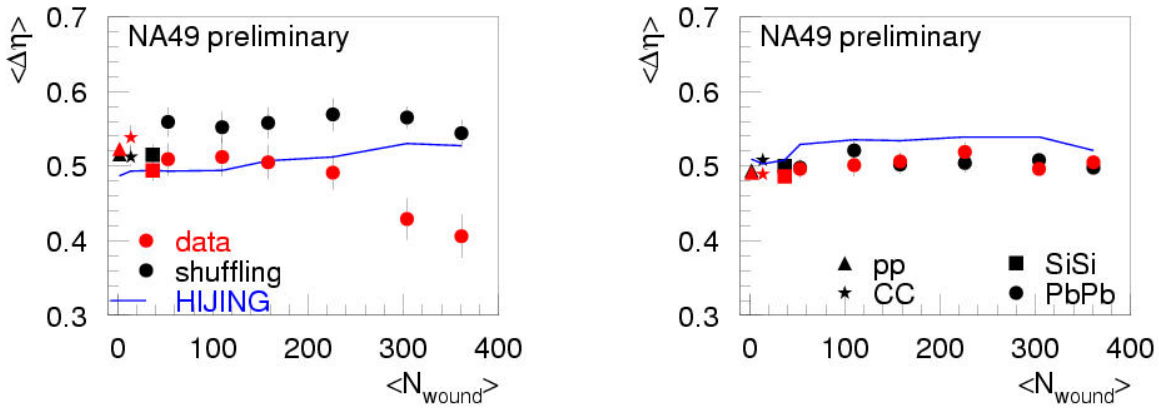

Figure 5. Width $\langle\Delta\eta\rangle$ of the balance function versus system size and centrality for charged particles at mid-pseudorapidity $2.5 < \eta < 3.9$ (left) and for forward pseudorapidities $4 < \eta < 5.4$ (right) in p+p and A+A collisions at 158A GeV.

3. ENERGY DEPENDENCE OF HADRON PRODUCTION

Motivated by the hypothesis [23] that the phase transition is first crossed between AGS and top-SPS energies, NA49 has measured hadron production in 5 energy steps from 20 to 158A GeV. A hadron gas analysis of the produced large set of hadron yields at each energy shows that towards lower energies the freeze-out temperature decreases while the baryochemical potential increases [4]. Comparing this smooth change of parameters with the phase boundary calculated from lattice QCD [6] it appears that for lower energies the systems at freeze-out start departing from this boundary.

An effect of the increasing baryon density is seen in the strong decrease of the $\overline{\mathrm{B}}$/B ratios towards lower energies (fig. 6). Although statistical models always reproduce the ordering by strangeness content and the overall energy dependence, a puzzling effect is hidden in this plot: the $\overline{\Lambda}/\overline{\mathrm{p}}$ ratio at midrapidity is close to/above 1 for all energies and even increases towards lower energies (fig. 7). These values can not be reproduced by statistical models. Whether an increased antiproton absorption at lower energies might be an explanation remains an open issue since the similar inverse slopes of the p_t-spectra measured for protons and antiprotons (fig. 10) are not expected in such a scenario.

As NA49 measures a large fraction of all strangeness carriers [27,28] the energy dependence of total strangeness production can be determined very accurately. The only extrapolations needed are either small (Ξ, Ω and antiparticles if not measured) and performed by using yields from the hadron gas model [4], or they are based on the assumption of isospin symmetry (K^0,$\overline{\mathrm{K}^0}$) and an empirical factor of $(\Sigma^{\pm} + \Lambda)/\Lambda = 1.6$ (to estimate the yield of $\Sigma^{\pm}$ and antiparticles) [29]. The sum of all (anti-)strange constituent quarks in the produced hadrons is presented in fig. 8. As expected from strangeness conservation one observes an agreement between the multiplicities of s and $\bar{\mathrm{s}}$ quarks. This result represents an important check of the internal consistency of the NA49 data. Furthermore, fig. 8 demonstrates that the increase of strangeness production with energy slows down at about 30A GeV. Also the rate of increase of pion production grows slightly in this region [28]. Therefore, a maximum of the relative strangeness production is obtained around

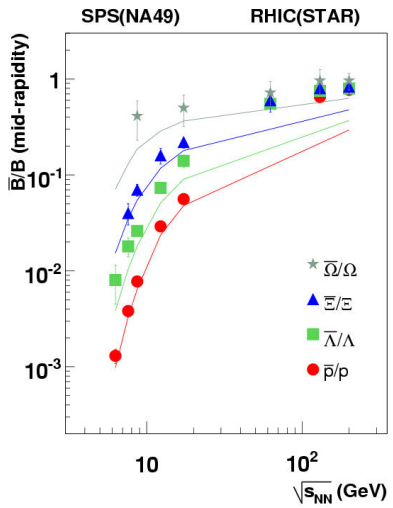

Figure 6. $\overline{\mathrm{B}}/\mathrm{B}$ ratio at midrapidity versus energy. The lines show the ratio from a hadron gas model fit to 4π data including a strangeness undersaturation factor γ_s [24].

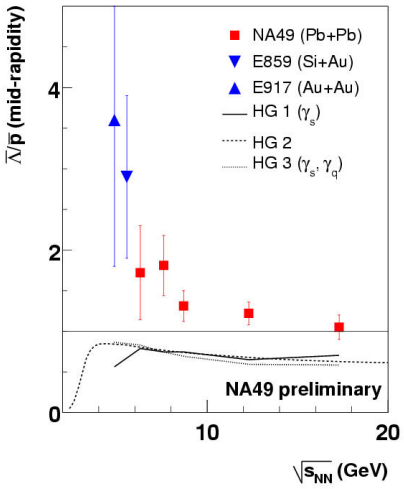

Figure 7. $\overline{\Lambda}/\overline{\mathrm{p}}$ ratio at midrapidity versus energy ($\overline{\Lambda}$ not corrected for contributions from $\overline{\Xi}$ decay). The lines show the ratio from hadron gas model fits to 4π data: HG 1 including γ_s [24], HG 2 without it [25], HG 3 including γ_s and γ_q [26].

this energy (fig. 9) while for higher energies extending up to RHIC the ratio remains stable (not shown). Although the rapid increase followed by a saturation is described by statistical hadron gas models [5,25] assuming a smooth change of temperature and baryochemical potential and full strangeness saturation (γ_s=1), such a distinct maximum cannot be explained. Also microscopic transport models such as UrQMD and HSD fail to describe this observation [30]. On the other hand, the maximum at about 30A GeV was predicted as a signal of the onset of deconfinement [23].

Additional support for a change in the production mechanism for hadrons in the lower SPS energy range comes from the investigation of p_t-spectra. Fig. 10 presents the energy dependence of mean transverse masses for pions, kaons and protons. All show a steep rise followed by a flattening in the same range in which the change in total and relative strangeness production is observed. Where measured, transverse masses agree well for particles and their antiparticles. Such a step-like behavior is not explained by microscopic transport calculations [30] but is consistent with assuming a first order phase transition with the corresponding change of the equation of state [31].

The study of particle correlations might reveal more information about the hadronization process. Fig. 11 shows new results from an analysis of the energy dependence of the width of the balance function of charged particles at midrapidity. In order to compare the different energies, the width of the balance function is normalized to shuffled events in which all correlations are removed and for which the width has its maximum value allowed by charge conservation. This way the acceptance dependence of the measurement is largely removed. W would increase for a decreasing width of the balance function

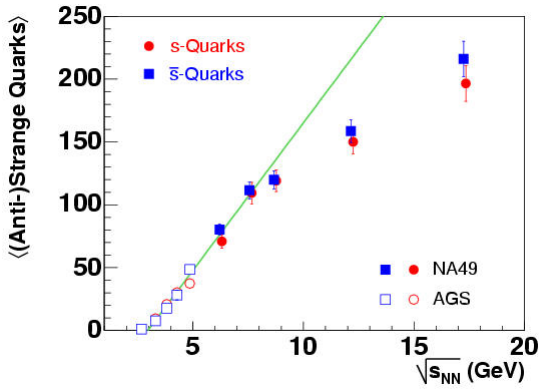

Figure 8. Energy dependence of total multiplicity of (anti-)strange constituent quarks (s-quarks: K^+, $\overline{K^0}$, Λ including Σ^0, Ξ, Ω, and $\Sigma^{\pm}$; antiparticles for $\bar{s}$-quarks) [29]. The line gives a linear extrapolation of the yields at low energies.

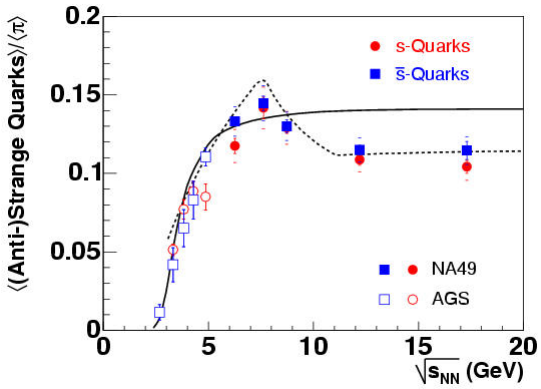

Figure 9. Relative strangeness production versus energy [29]. The solid line shows a statistical hadron gas calculation with a smooth change of T and μ_B and $\gamma_s = 1$ [25], the dashed line a prediction assuming a first order phase transition to a partonic phase at 30A GeV beam energy [23].

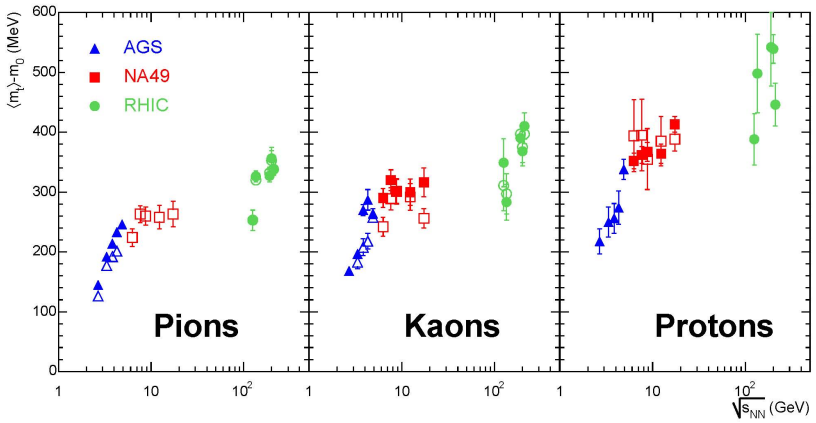

Figure 10. Energy dependence of $\langle m_t \rangle - m_0$ for π^+, K^+, p (full symbols) and their antiparticles (open symbols) [29].

predicted for delayed hadronization. Fig. 11 shows that W increases with energy, with possibly a plateau in the SPS energy range. However, before interpreting these results in terms of such a model, a more thorough investigation of the effect of using different phase space windows at each energy is needed.

The balance function is largely dominated by mesons, whereas a coalescence analysis of deuterons and protons can provide information on coherence volumes for baryons. The coalescence parameter B_2 determined from (anti-)deuteron and (anti-)proton spectra is inversely correlated to the coherence volume [32]. A continuous decrease of B_2 and thus an increase of the correlation volume is observed towards higher energies for both, particles and antiparticles (fig. 12).

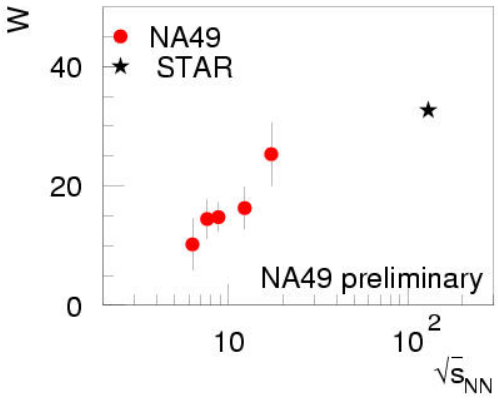

Figure 11. Energy dependence of the normalized decrease of the width of the balance function $W = \left(\frac{\langle\Delta\eta\rangle_{\rm shuffling} - \langle\Delta\eta\rangle_{\rm data}}{\langle\Delta\eta\rangle_{\rm shuffling}}\right) \cdot 100$ for charged particles at mid-pseudorapidity (window of 1.4 units, center of pseudorapidity range slightly forward shifted).

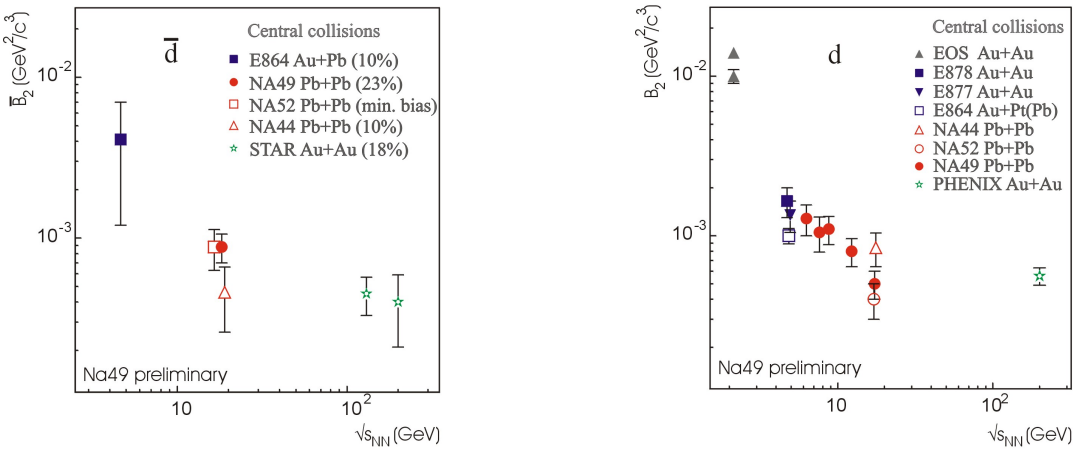

Figure 12. Energy dependence of the coalescence parameter B_2 calculated from (anti-) deuteron and (anti-)proton spectra.

4. SUMMARY AND CONCLUSION

NA49 has systematically investigated the dependence of hadron production on system-size, centrality and energy, the former in particular at the top-SPS beam energy of 158A GeV, the latter mostly for central Pb+Pb collisions. At top-SPS energies, strongly interacting matter of high energy density is created in central Pb+Pb collisions and the hadrochemical freeze-out occurs close to the predicted phase boundary. For collisions of nuclei with smaller A or for peripheral Pb+Pb reactions, the results are consistent with assuming the creation of several smaller systems and an earlier freeze-out. For a large set of observables it was shown that the created matter behaves in a similar manner as observed at RHIC. However, when decreasing the beam energy, distinct changes in hadron production properties are observed around 30A GeV. Although the strongly increasing baryon density clearly influences particle production, the observed structures can best be explained by models assuming the onset of deconfinement at the lower SPS energies.

REFERENCES

1. S. Afanasiev et al., Nucl. Instr. Meth. A 430 (1999) 210.
2. K. Werner, Phys. Rep. 232 (1993) 87.
3. T. Alber et al., Phys. Rev. Lett. 75 (1995) 3814.
4. F. Becattini et al., Phys. Rev. C 69 (2004) 024905.
5. P. Braun-Munzinger et al., Nucl. Phys. A 697 (2002) 902.
6. Z. Fodor and S.D. Katz, JHEP 0404 (2004) 050.
7. J. Cleymans et al., Phys. Rev. C 71 (2005) 054901.
8. R. Stock, Phys. Lett. B 456 (1999) 277.
9. P. Braun-Munzinger, J. Stachel, and C. Wetterich, Phys. Lett. B 596 (2004) 61.
10. C. Alt et al., Phys. Rev. Lett. 94 (2005) 052301.
11. S.S. Adler et al., Phys. Rev. C 69 (2004) 034909.
12. S. Hamieh, K. Redlich, and A. Tounsi, Phys. Lett. B 486 (2000) 61.
13. C. Höhne, F. Pühlhofer, and R. Stock, hep-ph/0507276.
14. E.G. Ferreiro, F. del Moral, and C. Pajares, Phys. Rev. C 69 (2004) 034901.
15. T. Anticic et al., Phys. Rev. C 70 (2004) 034902.
16. St. Mrowczynski, M. Rybczynski, and Z. Wlodarczyk, Phys. Rev. C 70 (2004) 054906.
17. S.S. Adler et al., Phys. Rev. Lett. 93 (2004) 092301.
18. J. Adams et al., Phys. Rev. Lett. 90 (2003) 172301.
19. C. Alt et al., Phys. Rev. C 71 (2005) 034903.
20. I. Kraus for the NA49 collaboration, J. Phys. G: Nucl. Part. Phys. 31 (2005) S147.
21. G. Stefanek for the NA49 collaboration, this volume.
22. A. Laszlo for the NA49 collaboration, this volume.
23. M. Gazdzicki and M. Gorenstein, Acta Phys. Polon. B 30 (1999) 2705.
24. J. Manninen, F. Becattini, and M. Gazdzicki, in preparation.
25. J. Cleymans and K. Redlich, Phys. Rev. Lett. 81 (1998) 5284 and K. Redlich, private communication.
26. J. Letessier and J. Rafelski, nucl-th/0504028.
27. S.V. Afanasiev et al., Phys. Lett. B 538 (2002) 275; S.V. Afanasiev et al., Phys. Rev. C 66 (2002) 054902; T. Anticic et al., Phys. Rev. Lett. 93 (2004) 022302; C. Alt et al., Phys. Rev. Lett. 94 (2005) 192301.
28. M. Gazdzicki for the NA49 collaboration, J. Phys. G: Nucl. Part. Phys. 30 (2004) S701.
29. C. Blume for the NA49 collaboration, J. Phys. G: Nucl. Part. Phys. 31 (2005) S685.
30. E.L. Bratkovskaya et al., Phys. Rev. C 69 (2004) 054907.
31. L. Van Hove, Phys. Lett. B 118 (1982) 138; M. Gorenstein et al., Phys. Lett. B 567 (2003) 175; Y. Hama et al., Braz. J.Phys. 34 (2004) 322.
32. L.P. Csernai and J.I. Kapusta, Phys. Rep. 131 (1986) 223; T. Anticic et al., Phys. Rev. C 69 (2004) 024902.